Quaternary International xxx (xxxx) xxx

Contents lists available at ScienceDirect

Quaternary International

journal homepage: www.elsevier.com/locate/quaint

Geological, paleoenvironmental, and depositional dynamics at the Middle Pleistocene *Palaeoloxodon antiquus*-bearing site of Campo della Spina, Central Italy

Paul P.A. Mazza [a,*], Fabrizio Marra [b], Giovanni Maria Di Buduo [c], Luca Bellucci [d], Mirko Bonechi [e], Ezra Goemans [e], Cosimo Bonechi [e], Luca Costantini [c], Sebastien Nomade [f], Danilo M. Palladino [g], Alison Pereira [h], Andrea Savorelli [d]

[a] *Dipartimento di Scienze della Terra, Università degli Studi di Firenze, via La Pira, 4, 50121, Florence, Italy*
[b] *Istituto Nazionale di Geofisica e Vulcanologia, Rome, Italy*
[c] *Museo Geologico e delle Frane di Civita di Bagnoregio, Viterbo, Italy*
[d] *Museo di Geologia e Paleontologia, Università degli Studi di Firenze, via La Pira, 4, 50121, Florence, Italy*
[e] *Tacheolab S.r.l., Via della Comunità Europea, 22, 50063, Figline Valdarno, Florence, Italy*
[f] *CEA-CNRS, UMR 8212, Laboratoire des Sciences du Climat et de l'Environnement, CEA-UVSQ et Université Paris Saclay, Bat 714, Orme des Merisiers, 91191, Gif sur Yvette, France*
[g] *Dipartimento di Scienze della Terra, Sapienza-Università di Roma, Rome, Italy*
[h] *Laboratoire GEOPS, UMR 8148, Université Paris-Saclay, bâtiment 504, 1 rue du Belvédère, 91400, Orsay, France*

ARTICLE INFO

Keywords:
Straight-tusked elephant
Quaternary
MIS 11
Latium
Taphonomy
Climate dynamics

ABSTRACT

The paleontological site of "Campo della Spina", in central Italy, offers valuable insights into Middle Pleistocene paleoenvironments. Excavations revealed well-preserved skeletal remains of an adult *Palaeoloxodon antiquus*, embedded in a sedimentary lens displaying alternating lacustrine and volcanoclastic flow characteristics. The well-preserved state of the remains suggests the elephant died at the site where it was found and was subsequent buried under conditions that facilitated preservation, while evidence of bone breakage and disarticulation indicates potential post-depositional disturbance, likely attributable to tractive water movements or debris flow events. These findings provide interdisciplinary research opportunities, shedding light on past climate dynamics and depositional processes. The site's significance lies in its contribution to understanding rapid aggradation, volcanic activity impacts, and climatic transitions during Marine Isotope Stages (MIS) 11- 9 intervals. The study highlights the importance of paleoclimate studies for informing contemporary climate change mitigation strategies. Overall, Campo della Spina offers a unique window into the interplay between climate dynamics, geological processes, and paleoenvironments, with implications for understanding past environmental changes and informing future conservation efforts.

1. Introduction

Northern Latium, central Italy, has emerged over the years as a region of appreciable scientific interest for paleontological exploration (Aureli et al., 2015; Boschian et al., 2018; Marra et al., 2018, and references therein). Recent studies (Marra et al., 2019; Di Buduo et al., 2020) have elucidated the geological history of this region, particularly in relation to the Middle Pleistocene. These investigations have reconstructed a succession of fluvial terraces and established geochronological constraints on the sedimentary deposits, revealing a direct correlation between sedimentation and phases of sea-level rise during the Middle Pleistocene glacial terminations (Marra et al., 2018; 2016, and ref. therein). In particular, $^{40}Ar/^{39}Ar$ ages of both primary and reworked volcanic deposits interbedded with the sedimentary deposits have enabled Marra et al. (2019) to identify three aggradational successions deposited during the sea-level high stands of Marine Isotope Stages (MIS) 9, 7 and 5. These sedimentary successions comprise a suite of terraces formed through the interplay of glacio-eustatic fluctuations, sedimentary processes, regional uplift, and fault displacement associated primarily with volcano-tectonic activity at the Bolsena and Latera

* Corresponding author.
E-mail address: paul.mazza@unifi.it (P.P.A. Mazza).

https://doi.org/10.1016/j.quaint.2024.10.014
Received 31 May 2024; Received in revised form 2 October 2024; Accepted 23 October 2024

calderas (333-110 ka, Palladino et al., 2010; Acocella et al., 2012; Marra et al., 2020a, 2020b; Monaco et al., 2021).

In the area under investigation, the combination of intense volcanic activity and proximity to the sea during the Middle Pleistocene, preceding regional tectonic uplift (Marra et al., 2019; Di Buduo et al., 2020), created favorable conditions for the selective transport, deposition, and preservation of fossil remains. During periods of sea-level decline, increased stream momentum facilitated the selective transport and accumulation of bones in valley bottoms. Subsequent rapid infilling of these incisions by fluvial-lacustrine sedimentary deposits, driven by sea-level rise during glacial terminations and often accompanied by the sudden emplacement of primary or secondary volcanoclastic-flow deposits, sealed the fossil assemblages and provided optimal conditions for their preservation.

Numerous paleontological discoveries of mammalian remains have been documented in the eastern sector of the Vulsini Volcanic District, with some of the earliest records dating back several centuries (Ciampini, 1688). Clerici (1895, 1908) mentions the presence of mammal remains in Marquis Gualterio's private collection, collected from various sites.

Throughout history, only a limited number of studies have been conducted on specific sites or remains, with some merely reporting the discovery of bones (Brocchi, 1816; Pianciani, 1817; Clerici, 1895, 1908; Trevisan, 1948; Palombo and Villa, 2003; Mancini et al., 2004). Remains of various genera and species, from Lower through Upper Pleistocene deposits, but predominantly from the Middle Pleistocene, have been recovered over the years from several localities in the vicinity of Civitella d'Agliano, Lubriano, Rio Fratta, Graffignano, Grotte Santo Stefano, Castel Cellesi, Bagnoregio, Gallese, and Roccalvecce (Marano and Palombo, 2014; Marra et al., 2019). These fossils were found in alluvial sediments, primarily diatomaceous, intercalated with volcanic deposits, as well as in thick sedimentary units associated with sea-level high-stands.

Significant discoveries include those from the area of Grotte Santo Stefano, approximately 6 km south of the area studied for the present research, where two nearly complete skeletons of *Palaeoloxodon antiquus* were unearthed from diatomaceous layers in the past (Trevisan, 1948; Palombo and Villa, 2003). These specimens are currently on display at the Museo Civico di Storia Naturale ''Giacomo Doria'' in Genoa and at the MUST - Museo Universitario di Scienze della Terra of the "Sapienza, University of Rome".

Among the notable findings in this region is the discovery of a *Palaeoloxodon antiquus* skeleton at Campo della Spina, near Castel Cellesi, in the municipality of Bagnoregio, province of Viterbo (Fig. 1).

The specimen is the object of the present study. Exploration of this paleontological site was conducted in 2013 following the chance discovery of isolated skeletal parts of an adult individual along an unpaved road. This initial report led to an excavation in 2014, exposing a concentration of disarticulated bones. The 2014 systematic excavation offered the opportunity to organize a paleontology summer field school (Mazza, 2014).

The excavation at Campo della Spina carries particular importance beyond its immediate paleontological significance. The study of its *Palaeoloxodon antiquus* and of its depositional context offers interesting insights into Middle Pleistocene environments, which can contribute to a better understanding of long-term climate interactions and potentially inform models of future climate evolution.

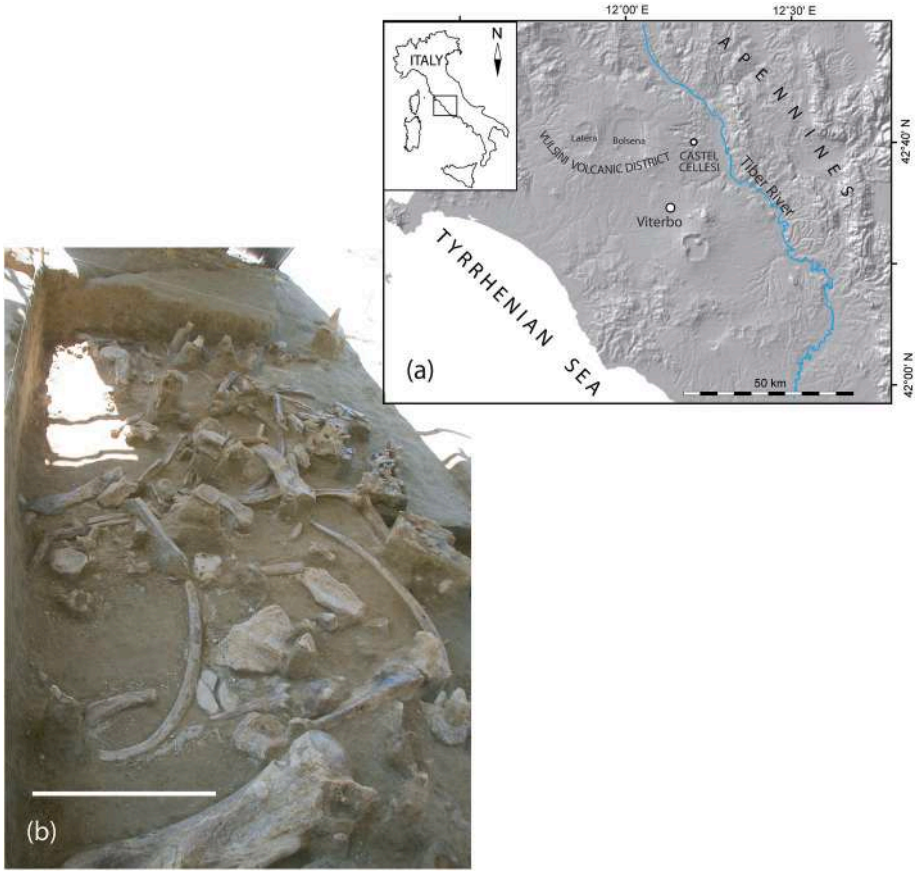

Fig. 1. Location of the site.(a). Map showing the location of the Campo della Spina excavation site; Paleontological sites mentioned in the text: 1 Lubriano, 2 Civitella d'Agliano, 3 Graffignano, 4 Roccalvecce, 5 Grotte S. Stefano, 6 Gallese, 7 Cava Rio Fratta. (b). Overview of the site from North-North-East. Bar scale in (b): 50 cm. With permission from the Italian Ministry of Culture (MiC) – Superintendence for Archaeology, Fine Arts, and Landscape for the Province of Viterbo and Southern Etruria.

2. Methods

2.1. Excavation techniques

Archaeologists and paleontologists typically employ Cartesian coordinates x, y, z to spatially locate discovered elements (e.g., Anemone et al., 2011). However, in the Campo della Spina excavation, a modified approach has been adopted, using only two-dimensional Cartesian coordinates (x, y) and determining the third vertical coordinate through 3D scanning. This method aligns with the conventional practice of horizontal excavation. The excavation area was oriented in the NW-SE direction. The designated site was systematically subdivided into a grid of squares, each with a length of 1 m, and excavation followed the established criterion of "peeling" (e.g., Harris, 2014). This approach entailed the methodical removal of sediments from successive levels encountered during the excavation process. The levels encountered in stratigraphic succession from top to bottom were numerically designated as Stratigraphic Units (SUs). Quadrants within the site were alphabetically designated from A to D, proceeding from west to east, and numerically from 1 to 8, proceeding from north to south. The adoption of 3D scanning aimed to obtain a more reliable and precise documentation of the entire extent of the investigated SUs (Fig. 2).

At the time of excavation (June 2014), the instrumentation and methodology employed were advanced with respect to traditional surveying methods. Indeed, a series of high-definition scans were performed with a point cloud colored with RGB data. A state-of-the-art instrument for the time was employed: a Leica P40 Laser Scanner. Using a 3D laser scanner, it was possible to fully capture a 360° view with 12 scans of the entire environment surrounding the scan points arranged radially around the excavation to eliminate, as much as possible, shadow cones formed, for example, in the sub-squares. The point clouds, equipped with x, y, z coordinates and chromatic references, were related through a compensated polygonal network to nullify topographic error (Ghilani, 2010). With the aid of dedicated software Cyclone (Leica Geosystems, Switzerland) and 3Dreshaper (Technodigit, France), a textured 3D mesh model was obtained with ground-based photogrammetry implementation, allowing for perfect geometric and paleontological surface reconstruction. The advantages of this methodology, now widely embraced in the archeological realm (Mumtaz, 2008; Campana et al., 2012; Held, 2012), included a perfectly detailed geometric reconstruction of the excavation surface, with an unprecedented amount of information and extremely rapid execution times. A dimensioned planivolumetric drawing, which combines both planar and volumetric aspects, was prepared, overlaid onto various types of orthographic projection views of the colored point cloud with different levels of transparency, along with an orthophoto of the textured mesh, as well as some sections. This constitutes the most comprehensive representation of the examined areas. Thus, this modeling proves to be a highly effective and appropriate technique for capturing, documenting, and presenting excavated paleontological heritage. This method holds significant potential for enhancing the overall quality of recorded excavation data. The provision of high-resolution geometric details facilitates direct quantification of the collected information.

2.2. Paleobiological and taphonomic analysis of the Campo della Spina elephant

The elephant skeleton is incomplete (Figs. 1–3). Measurements of the measurable skeletal elements were taken according to the methods outlined by Lister (2021), which were adapted from Göhlich's (1998) protocols. Molar plate (lamellar) frequency was assessed per 10 cm (Davies, 2002). Epiphyseal fusion occurs at specific stages throughout an elephant's lifespan and corresponds with the timing of tooth eruption. Therefore, the ontogenetic age of the Campo della Spina skeleton was estimated by combining observations of dental eruption and wear patterns with the degree of epiphyseal fusion in the limb bones. Reference for all this was made to Rensch (1959), Laws (1966), Blueweiss et al. (1978), Roth (1984), Lister (1994, 1999), Lister et al. (2012), and Larramendi et al. (2020).

The absence of sexually diagnostic bones (i.e., the atlas, axis, and especially the pelvis), as well as skeletal features typically associated with sexual dimorphism in *Palaeoloxodon antiquus* (Roth, 1984; Kroll, 1991; Averianov, 1996; Lister, 1994; 1999; Todd, 2010; Haynes, 2017), makes determining the sex of the Campo della Spina elephant remains

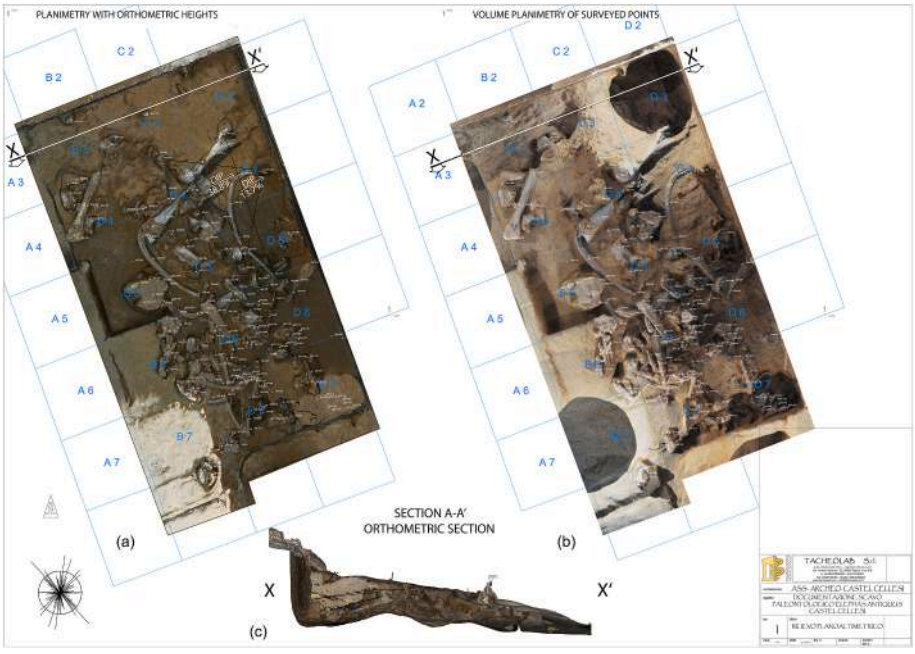

Fig. 2. Digitally generated documentation of the Campo della Spina excavation. (a). Planimetry with indication of orthometric heights of each specimen. (b). Surveyed points in volume plan view. (c): Excavation section through X-X'. A rose diagram in the lower left of the figure displays the direction and percentage of spatial orientation of elongated specimens, indicating a highly random arrangement of the remains.With permission from the Italian Ministry of Culture (MiC) – Superintendence for Archaeology, Fine Arts, and Landscape for the Province of Viterbo and Southern Etruria.

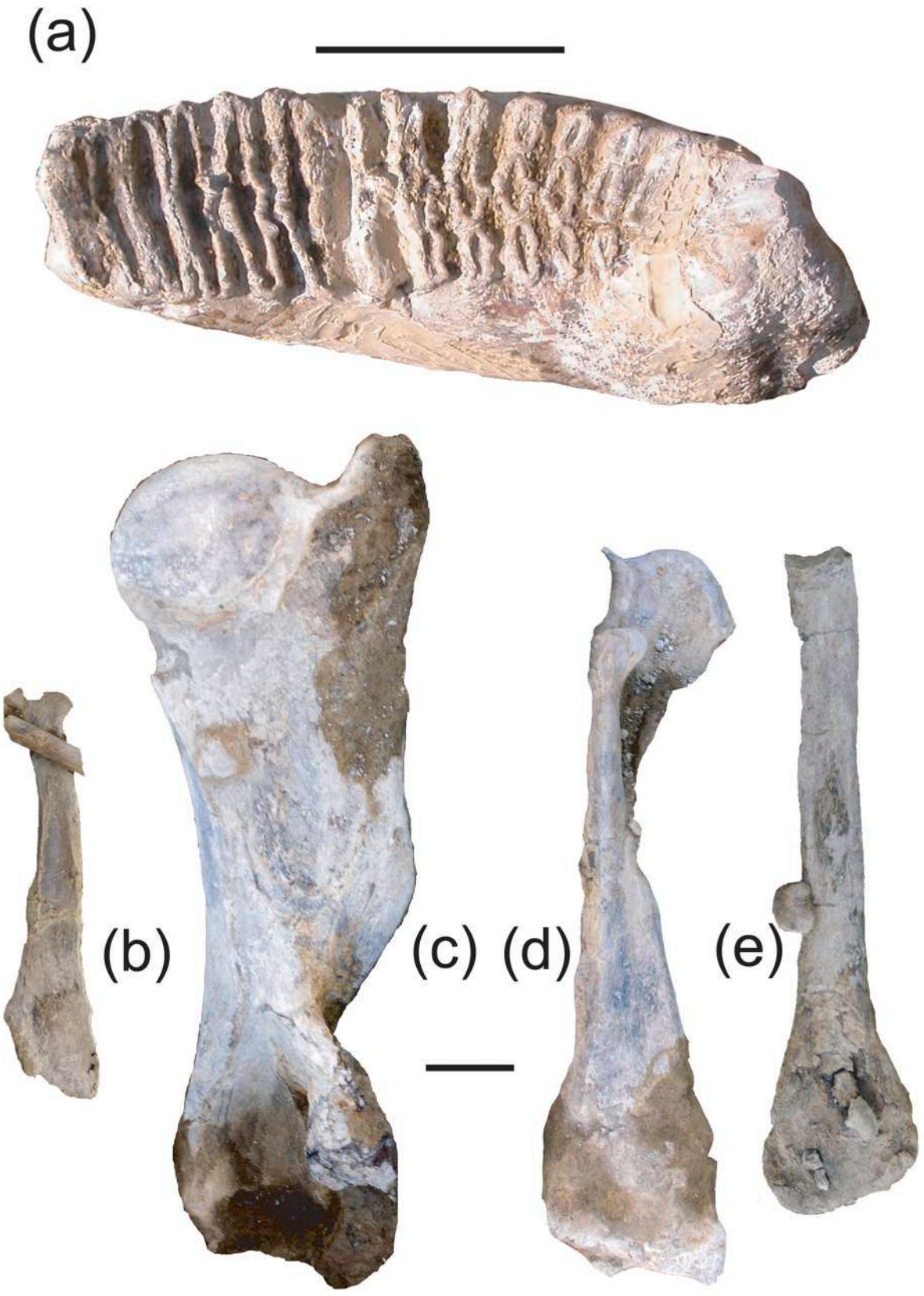

Fig. 3. Selected *Palaeoloxodon antiquus* remains from the site of Campo della Spina. (a). Left lower m3, occlusal view. (b). Right first rib. (c). Incomplete right humerus, caudal view. (d). Incomplete right ulna, dorso-medial view. (e). Right radius, dorso-medial view. Scale bar: (a). 20 cm, (b–e). 10 cm. With permission from the Italian Ministry of Culture (MiC) – Superintendence for Archaeology, Fine Arts, and Landscape for the Province of Viterbo and Southern Etruria.

particularly challenging. The individual's sex could only be hypotesized indirectly through body size estimates referring to Lister and Stuart's (2010) and Larramendi's (2016) protocols.

The taphonomic analysis commenced with the anatomical and taxonomic identification of the specimens. Protocols outlined by Haynes (1983) and Villa and Mahieu (1991) were consulted to discern whether the bones had incurred breakage in a fresh or dry state. Evaluation of potential pre- and post-depositional alterations included scrutiny for evidence of carnivore-ravaging, trampling, root or humic-acid etching, abrasion/polishing, as well as weathering with reference to Behrensmeyer's (1978). Additional procedures were implemented to extract specific biological insights about the elephant.

2.3. $^{40}Ar/^{39}Ar$ dating

Ar/Ar analyses were conducted at the dating facility of the Laboratoire des Sciences du Climat et de l'Environnement (CEA, CNRS UMR 8212, Gif-sur-Yvette, France). Samples underwent initial crushing, sieving, and washing in distilled water. Approximately 40 transparent K-feldspars and feldspathoids (sanidine and leucite), ranging in size between 500 μm and 1 mm, were manually selected under a binocular. Prior to irradiation, crystals were leached for 5 min in a 10% HF solution to remove potential groundmass pieces and surface alteration phases.

Around twenty-five crystals from each sample underwent irradiation in the Cd-lined, in-core CLICIT facility of the Oregon State University TRIGA reactor in two separate irradiation sessions: IRR. CO-017 (1 h) for CC-9, CC-10, CC-11, and IRR. CO-019 (1 h) for CC-17. Interference corrections were based on nucleogenic production ratios from Balbas et al. (2016). Post-irradiation, crystals were placed into a copper 133-pit sample holder within a Teledyne Cetac differential vacuum window connected to a custom-designed compact extraction line.

Sequentially, minerals were fused one by one using a 100 W Teledyne Cetac CO_2 laser for 15 s at 2.5 W. Prior to fusion, each crystal underwent a 20-s sweep at 0.3 W to eliminate trapped gases and fractures. Extracted gases were purified first by a SAES GP 50 cold getter for 90 s, followed by two hot SAES GP 50 getters for 230 s. The five Argon isotopes (^{40}Ar, ^{39}Ar, ^{38}Ar, ^{37}Ar, and ^{36}Ar) were measured using a multicollector NGX 600 mass spectrometer equipped with 9 ATONA® amplifiers array and an electron multiplier. Further technical specifications regarding the NGX 600 ATONA detector array are detailed in Cox et al. (2020).

Isotopes ^{40}Ar, ^{39}Ar, ^{38}Ar, ^{37}Ar, and ^{36}Ar were collected simultaneously, while ^{37}Ar was measured separately. Each isotope measurement consisted of 15 cycles of 20-s integration time. Peak intensity data were processed using ArArCALC V2.4 (Koppers, 2002). Neutron fluence J factors were calculated using co-irradiated Alder Creek sanidine standard ACs-2 associated with an age of 1.1891 Ma (Niespolo et al., 2017), according to the K total decay constant of Rensch (1959) ($\lambda e.c. = (0.5757 \pm 0.016) \times 10- 10\ yr- 1$ and $\lambda\beta^{-} = (4.9548 \pm 0.013) \times 10- 10\ yr-1$)).

J-values were determined using 14 flux monitor crystals from pits framing the samples in each irradiation disk. The measured J-values are 0.0002824 ± 0.00000017 for CC-9 and CC-10, 0.0002840 ± 0.00000020 for CC-11, and 0.0002752 ± 0.00000022 for CC-17. To assess detector linearity, mass discrimination was monitored by analyzing at least 10 air shots of various beam sizes ranging from 1.0 10− 2 up to 5.0 10− 2 V (1–5 air shots). Approximately 15 air shot analyses were conducted daily, both before and after the unknown measurements. Discrimination was calculated based on the $^{40}Ar/^{36}Ar$ ratio of 298.56 (Lee et al., 2006). Procedural blank measurements were performed after every two to three unknowns, with typical 5-min time blank backgrounds ranging between 0.6 and 2.3 10− 4 V for ^{40}Ar and 20–50 cps for ^{36}Ar (equivalent to about 3.0–7 10− 7 V). Full analytical data for each sample are available in Supplementary Dataset 1 (SD-1).

3. Results

3.1. $^{40}Ar/^{39}Ar$ dating

Results are depicted as probability diagrams (Fig. 4). Weighted mean age uncertainties are reported at 2σ, encompassing both analytical and J-values uncertainties, and were computed using Isoplot 4.1 (Ludwig, 2003).

For CC-9, twenty-two single crystal ages (a mixture of leucites and sanidines) were acquired. The probability diagram for CC-9 illustrates a complex deposit influenced by multiple volcanic events (Fig. 4a). Single crystal ages range from approximately 444 to 504 ka. The youngest population identified statistically comprises three crystals, yielding a weighted average age of 444.7 ± 2.1 ka (MSWD = 0.35, P = 0.71), interpreted herein as the youngest eruption recorded and the maximum age of deposition for this sedimentary layer.

Regarding CC-17, fourteen single crystal ages (primarily sanidines with few leucites) were determined. The associated probability diagram displays multiple modes, with a juvenile mode centered around 400 ka (8/14 crystals, Fig. 4b). Despite notable xenocryst contamination, with crystal ages ranging from 414 to 439 ka, the juvenile crystal population yields a precise and statistically coherent weighted mean age of 401.6 ± 1.2 ka (MSWD = 0.63, P = 0.73), interpreted as the age of the pumice fall deposit.

In the case of CC-10, fifteen single crystal ages (mostly sanidines with few leucites) were obtained. After excluding four obvious xenocrysts (~416 and ~436 ka), a primary population of juvenile crystals, comprising eleven specimens, is identified (Fig. 4c). This main Gaussian juvenile population allows for the calculation of a precise and statistically coherent weighted mean age of 398.8 ± 0.8 ka (MSWD = 0.79, P = 0.64), interpreted as the age of the CC-10 pyroclastic fall deposit.

Lastly, for CC-11, thirteen single crystal ages (sanidine) were derived. After excluding two xenocrysts (~337 and ~341 ka), a predominant population of eleven crystals is observed (Fig. 4c). The main Gaussian juvenile crystal population facilitates the determination of a robust weighted mean age of 329.2 ± 0.6 ka (MSWD = 0.90, P = 0.53), interpreted as the eruption age of this pyroclastic fall deposit.

3.2. Chronostratigraphy

The sedimentary/volcanic succession exposed at Campo della Spina and the geochronological constraints provided by the dated samples are shown in the cross-section presented in Fig. 5.

The $^{40}Ar/^{39}Ar$ ages obtained from the volcanic layers enable the identification of two major sedimentary cycles, influenced by glacio-eustatic processes and correlated with MIS 11 and MIS 9. Specifically, ages of 445 ± 2 and 399 ± 1 ka derived from samples CC-9 and CC-10, respectively, collected at the base and top of a ca. 20 m thick succession of silty-clayey deposits with frequent volcanoclastic intercalations, emphasize a strong correspondence between its deposition and the phase of sea-level rise during MIS 11 (Fig. 5). In particular, the youngest crystal population, dated to 445 ± 2 ka, derived from the reworked volcanoclastic sample CC-9, serves as a *terminus post quem* (maximum age) for the time of deposition (hence represented as ≤ in Fig. 5). This finding aligns with the occurrence of glacial termination V shortly thereafter and underscores the close relationship between sediment aggradation and sea-level rise at the onset of MIS 11 (Lisiecki and Raymo, 2005; Tsedakis et al., 2010; 2022). Similar conclusions can be drawn from the sedimentary sample CC-17, which also provides a maximum age for the completion of sediment aggradation during MIS 11. This is supported by the absolute age of 399 ± 1 ka obtained from the primary volcanic sample CC-10, which sets a maximum duration for MIS 11 high-stand.

An unconformity boundary, marked by the deposition of coarse debris-flow deposits consisting of both volcanic and travertine fragments, indicates the occurrence of an erosive phase during MIS 10 low

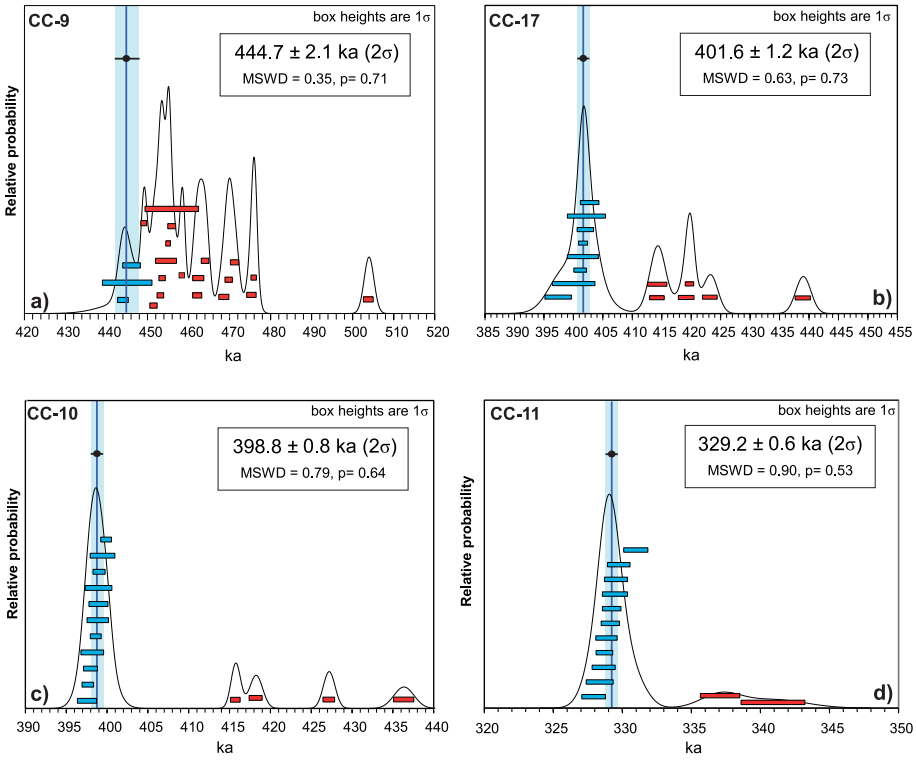

Fig. 4. Age probability diagrams of the $^{40}Ar/^{39}Ar$ experiments conducted on the four dated samples. MSWD: mean squared weighted mean; P: probability. See text for comments.

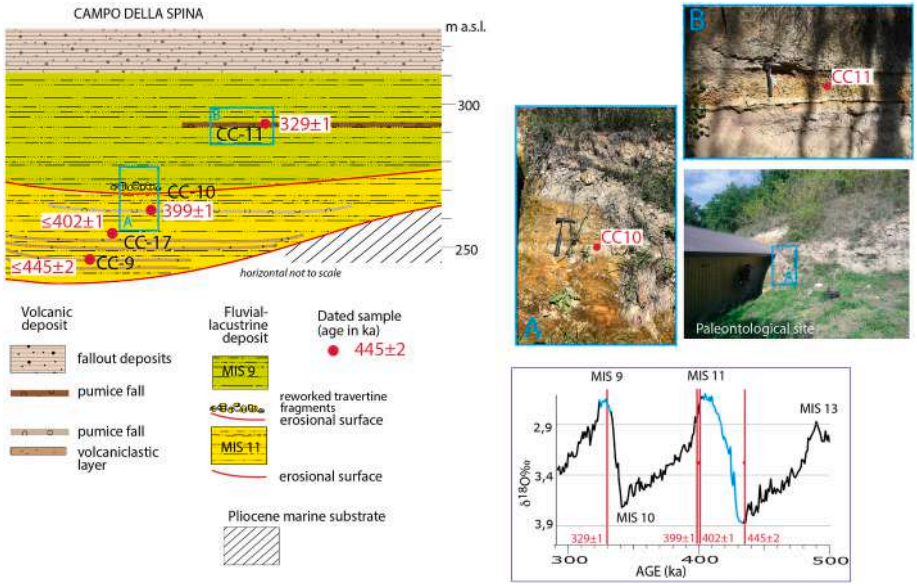

Fig. 5. Stratigraphic sketch and photographs of the sedimentary succession cropping out at Campo della Spina, displaying the position of the $^{40}Ar/^{39}Ar$ dated samples. Letters A and B indicate the positions of pictures A and B (blue rectangles) in the cross-section. The inset presents the age constraints on the sedimentary succession (red vertical bars) facilitating correlation with the $d^{18}O$ record of Lisiecki and Raymo (2005). See text for further comments and explanation.

stand (Fig. 5. The age of 329 ± 1 ka obtained from the pumice layer situated in the upper part of the overlying fluvial-lacustrine succession, approximately 30 m thick, provides evidence for the completion of aggradation of the new sedimentary succession during the MIS 9 high-stand.

The age derived from the youngest crystal population in the clay sample collected beneath the *Palaeoloxodon* remains enables a precise age constraint between 402 ± 1 and 399 ± 1 ka, corresponding to the very late aggradational phase during the high-stand of MIS 11 high stand.

3.3. Outline of the stratigraphic succession at the excavation site

The removal of approximately 5–8 cm of reworked road material (SU 1) exposed a silt-clayey ocherous layer (SU 2) (Fig. 6). This layer, primarily compact and massive, consists of reworked volcanoclastic

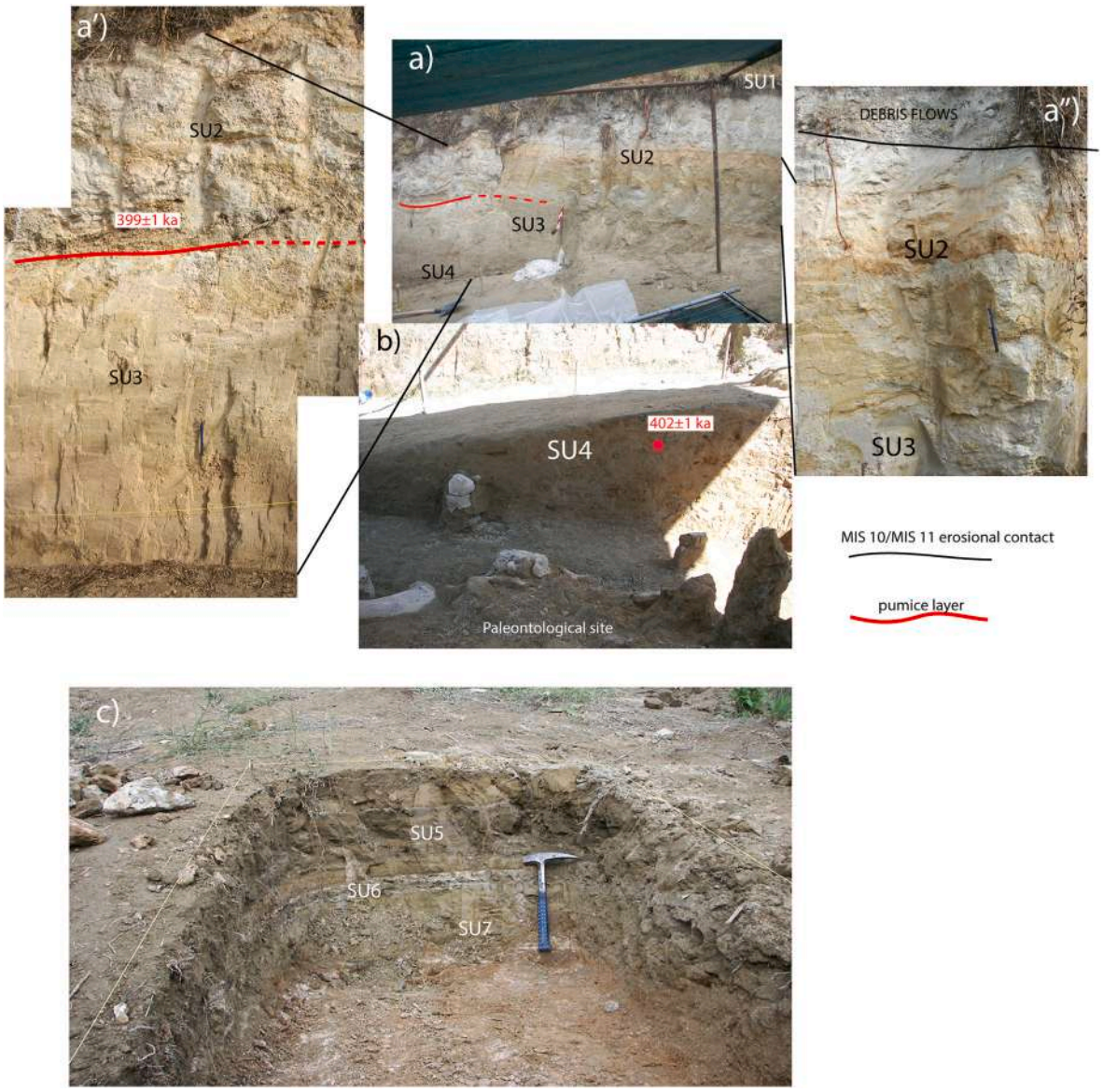

Fig. 6. Stratigraphic units and age constraints at Campo della Spina excavation. (a–c). Photographs of the Campo della Spina excavation site, showing (from top to bottom) the stratigraphic units (SU) forming the exposed sedimentary succession and the $^{40}Ar/^{39}Ar$ age constraints. (a'-a"). Detail of the upper part of the sedimentary succession. See text for description. With permission from the Italian Ministry of Culture (MiC) – Superintendence for Archaeology, Fine Arts, and Landscape for the Province of Viterbo and Southern Etruria.

material containing pumiceous lithoclasts and various other lithic elements. Additionally, it includes numerous vegetal remains of varying dimensions, rizoliths, small white gastropods with thin shells, and bioturbations. The sedimentary body, approximately 50–60 cm thick, rests upon a very hard and cemented lateritic duricrust, forming an irregularly patterned horizon. The duricrust delineates wide channels ranging from 16 to 90 cm and lies atop a sedimentary body akin to the overlying one, measuring approximately 90 cm in thickness (SU 3). Within this layer, a significant sedimentary lens, spanning 30–50 cm, contains gravel composed of various lithic elements, lightly rounded and poorly sorted, suspended within a grayish-top gray silty matrix (SU 4). The upper surface of this lens is notably disturbed, rising at various points with apices pointing upward, forming a series of flame-like structures. This lens constitutes the fossiliferous sedimentary body of the excavation, where bone remains were found partially submerged within and partially floating on this gray silty-gravel lens. All sedimentary bodies dip at an angle of 10° towards the North, with a North-South direction. Particularly, the gray silty-gravel fossiliferous lens decisively dips towards the D3 quadrant.

Reconstructing the stratigraphy from external outcrops surrounding the excavated perimeter, from the base upwards, the following layers are observed: 1) Approximately 20 cm of rhythmic gray clays, interspersed with fine sands containing quartz and volcanic minerals (the base of this level was not exposed) (SU 7); 2) 5 cm of light brown or white clayey marls with lentiform interbedded gray clays and fine sands containing quartz and volcanic minerals. This layer features plant remains, rizoliths, and ripple-marks (SU 6); 3) 30 cm of fine sands and laminated clays, occasionally exhibiting lenticular patterns, containing fragments of plant remains. This layer is notably characterized by a sandy base and top, separated by a laminated clay interbed with rhythmic patterns (SU 5); 4) Approximately 60 cm of compact light gray clayey silts, with reworked volcanoclastic material, lithoclasts of various compositions, numerous vegetal remains of varying dimensions, rizoliths, small white gastropods with thin shells, and bioturbations (SU 3); 5) Ferruginous duricrust; 6) Approximately 150 cm of compact ocherous clayey silts, similar to those underlying (SU2). Towards the upper part,

transitioning to the overlying stratigraphic term, a marked pedogenic reddening is observed; 7) Approximately 60 cm of white lacustrine diatomites. This layer features numerous plant remains, rizoliths, and some shells of small freshwater mollusks. Various channels with widths of 100–120 cm are present at the base (SU1).

3.4. The fossil record; paleobiological and taphonomic analysis

The fossil remains, which total 130 ranging from complete bones to fragment, were contained in SU 4, concentrated in quadrants A3, B3, B4, B6, B7, C3 to C5, C7, and D3 to D7 (Fig. 2). The skeletal and dental characteristics of the specimens match those of an elephant, with the exception of a deer rib fragment. Virtually all belong to a disarticulated skeleton of a large-sized individual.

The elephant skeleton is incomplete and disarticulated, but the bones are scattered randomly and closely associated (Fig. 2). The excavation exposed a premaxillary fragment, a fragment of right maxillary bone with molar, one cervical vertebra, eleven thoracic vertebrae, two or three lumbar vertebrae, a fragment of sacrum, many rib fragments, a complete right humerus, the distal end of left humerus, the right radius and ulna, part of what seems to be a tibia, the left fibula and a number of anatomically undetermined fragments. Although fragmentary, the specimens are in general well-preserved.

An isolated left lower molar (Fig. 3A)was the initial chance discovery made on the dirt road signaling the presence of the elephant. The tooth is one of the taxonomically most diagnostic elements of the skeleton. It is typically long and narrow, measuring approximally 33 cm in length and 8 cm in width, with no distal tapering, as seen in m3, and is in full wear. The molar exhibits 14–15 closely spaced enamel plates with heal, and a plate (lamellar) frequency of 5. Morphologically, individual plates display a characteristic oval or loop pattern of elongated enamel in occlusal view. The tooth's dimensions, along with the relationship between lamellar frequency and width, are consistent with *Palaeoloxodon antiquus* (Davies, 2002). With reference to "African Elephant Equivalent Years" (AEY), as recommended by Laws (1966), the Campo della Spina individual falls within the XXV to XXVII dental stage, suggesting an approximate age range of 50–60 years (Laws, 1966; Haynes, 2017).

Concerning skeletal fusion, humerus (Fig. 3C), radius/ulna (Fig. 3D, E), and fibula (=tibia) exhibit fused epiphyses, as do the vertebral plates. Female elephants are known to attain skeletal maturity earlier than males (Roth, 1984; Lister, 1999; Haynes, 2017). Nevertheless, the fully fused epiphyses of the Campo della Spina elephant prevent unequivocal sex determination based on the state of fusion of the postcranial elements. According to the insights of Roth (1984), Lister (1999), and Haynes (2017), complete epiphyseal fusion is achieved in female elephants aged between 50 and 60 years, as well as in males aged approximately 60–65 years.

The maximum lifespan is thought to be intricately linked to body size (Rensch, 1959; Blueweiss et al., 1978). Based on the allometric scaling proposed by Blueweiss et al. (1978), it is reasonable, thouogh not conclusive, to hypothesize that *Palaeoloxodon antiquus*, one of the largest extinct European proboscideans, may have had a lifespan approximately 10 years longer than contemporary elephants. While this remains speculative, it can be cautiously estimated that the Campo della Spina elephant may have reached an age of around 60–65 years at the time of its death.

Sexual dimorphism can aid in sexing the animal. Based on the equations proposed by Lister and Stuart (2010), and considering that the right radius of the Campo della Spina elephant measures 83 cm in length (Fig. 3,E) the individual's shoulder height is estimated to have ranged from 2900 to 3600 mm. With this shoulder height, and using Larramendi's (2016) protocols, the elephant's weight is estimated to have been less than 10,000 kg. These dimensions do not correspond to those typically associated with a male *Palaeoloxodon antiquus*, which may suggest the possibility that the specimen was a female individual.

In summary, integrating both dental and postcranial characteristics, it is deduced that the Campo della Spina elephant was likely aged 60–65 years at the time of its death. Additionally, considering its overall size and weight, there is a suggestion that the elephant may have been a female.

From the taphonomical viewpoint, the disarticulated bones of the *Palaeoloxodon antiquus* skeleton from Campo della Spina show evident bone to bone contact, with minimum films of sediment in between, and exhibit a bimodal orientation, aligning both in the NW-SE and NE-SW directions, indicating potential taphonomic post-depositional disturbance. The cortical surfaces reveal no signs of weathering or evidence of carnivore ravaging. The fracture surfaces of the broken skeletal parts exhibit characteristics consistent with fractures produced in a dry state, as defined by Haynes (1983) and Villa and Mahieu (1991). Conversely, trampling-derived scratches and grooves are notably limited.

4. Discussion

4.1. Depositional context

The state of preservation of the adult skeleton of *Palaeoloxodon antiquus* at Campo della Spina demonstrates a fortuitous combination of circumstances and agents that hindered the biostratinomic degradation of the animal's carcass and remains beyond a certain extent. This has facilitated the retention of numerous relevant insights into its paleobiology, while also providing valuable taphonomic and paleoenvironmental information.

The sedimentary succession hosting the fossil-bearing lens displays features characteristic of both lacustrine and debris flow environments, indicating a dynamic depositional setting influenced by fluctuating water levels and episodic sedimentary events. The absence of weathering or carnivore activity on the cortical surfaces of the elephant's bones, along with the lack of sediment between juxtaposed bone elements, suggests that the animal died *in situ*, with initial decomposition occurring in a protective environment. However, the compele disrticulation of the skeleton, coupled with the bimodal orientation of the separated bones, hints at later taphonomic post-depositional disturbance, potentially attributable to tractive water movements or debris-flow events.

The deposit encasing the fossil remains exhibits distinct characteristics of a volcanoclastic debris-flow (e.g., Vallance, 2005). This deposit is marked by abundant, cm-sized, gray and dark brown volcanic scoria clasts, which have accumulated at the base of a lenticular mudflow (Fig. 7a). At its base, the deposit is clast-supported (Fig. 7b–b'), with a ca. 40 cm-thick horizon comprised of scoria clasts displaying a fining upward sorting, accompanied by a gradual increase in a light brown-reddish clay matrix. This clay matrix constitutes the upper 50–60 cm of the deposit, which is devoid of volcanic fragments.

Some degree of bone breakage in a dry state, albeit without significant grooving or scratching of the bone surfaces, implies potential trampling, possibly mitigated by the protective environment provided by the sediments.

4.2. Paleoclimatic inferences

The observations above support the interpretation of a local depression which created hydraulic gradients leading to episodic water movements, likely associated with seasonal cycles of mixing and stratification. These movements may have been linked to seasonal hydrological cycles of thermal stratification (formation of distinct water layers) and mixing (redistribution of water and sediment during turnover). The fossil-bearing succession is embedded within a complex sequence of fluvio-lacustrine-pyroclastic deposits, reflecting a diverse geological history encompassing volcanic activity, sedimentation, and tectonic processes. The radiometric dating of the volcanic deposits preciselybrackets the fossil-bearing succession within the MIS 11 – MIS 9 interval. The ca. 400 ka dating of the fossiliferous level correlates it with

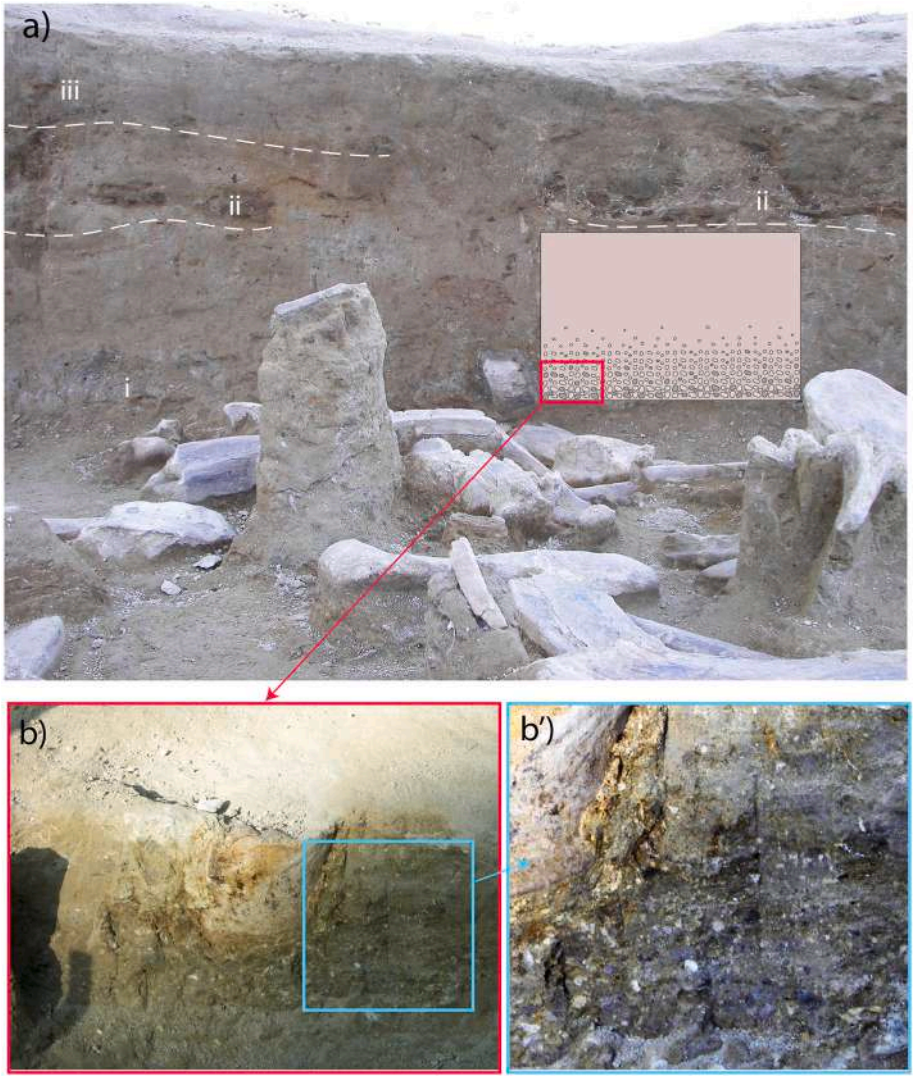

Fig. 7. Details of the excavation site. (a). Photograph of the excavation site exhibiting *Palaeoloxodon* remains embedded within the coarse-grained, volcanoclastic basal portion of the lowest debris flow among a series (i, ii, iii) exposed in the trench wall. Drawing reproduces the fining-upward volcanoclastic basal portion of the fossil-bearing debris flow. (b-b'). Close-up detail. With permission from the Italian Ministry of Culture (MiC) – Superintendence for Archaeology, Fine Arts, and Landscape for the Province of Viterbo and Southern Etruria.

substage MIS 11c.

Quaternary interglacials have garnered significant attention in the scientific community, primarily due to their crucial role in elucidating the potential trajectory of the Holocene in the absence of anthropogenic impact. Among these interglacials, MIS 11 stands out as particularly noteworthy. This heightened focus on MIS 11 stems from its characteristics, which sometimes lead it to be considered a suitable analog for the Holocene (de Abreu et al., 2005; Tzedakis, 2010; Zhao et al., 2019; Tzedakis et al., 2022). Both MIS 11 and the Holocene were marked by warm stages driven by low eccentricity peaks (Berger and Loutre, 2002; Loutre and Berger, 2003; Droxler et al., 2003; Dickson et al., 2009; Tzedakis, 2010). Consequently, MIS 11 is recognized as one of the pivotal interglacial stages of the past 450,000 years.

The characteristics of MIS 11 further contribute to its significance. For instance, the reconstructed extent of global ice sheet loss during MIS 11, along with late interglacial abrupt events and prolonged warmth (Candy et al., 2014) hold implications for the future of the current interglacial period. Understanding these aspects of MIS 11 provides valuable insights into past climatic conditions and helps to inform our understanding of future climate scenarios. Therefore, the study of MIS 11 plays a crucial role in advancing our knowledge of Quaternary climate dynamics and their relevance for contemporary environmental challenges.

Presently, there exists an extensive array of evidence detailing MIS 11 paleoclimates and paleoenvironments derived from marine, ice core, lacustrine, and terrestrial sequences. Several researchers (e.g., Prokopenko et al., 2001; Ashton, 2010; Fawcett et al., 2011; Railsback et al., 2015) subdivide MIS 11 into five phases (e, d, c, b, a), supplementing the traditional three substages (a, b, and c) (e.g., Tzedakis et al., 2001, 2012; Candy et al., 2014; Kleinen et al., 2014) - although de Abreu et al. (2005) and Westaway (2010) had found no justification for distinguishing any substages in MIS 11. Despite some viewpoints suggesting that MIS 11c may not have been an exceptionally warm "super interglacial" (*sensu* Melles et al., 2012), on the whole, MIS 11 is considered to mark the onset of a succession of interglacial periods, many of which rival or surpass the current warmth levels (EPICA community members, 2004; Blain et al., 2021). More specifically, recent opinions (e.g., Sassoon et al., 2023) are converging to recognize MIS 11c as the longest (approximately 426 to 400 ka), most humid, rather rainy, and warmest substage (e.g., Kandiano et al., 2012; Williams, 2019).

Over the past decade, research has largely confirmed previous notions regarding MIS 11c as a prolonged warm interval lasting 25,000 to

30,000 years. Additionally, investigations have reinforced the idea that MIS 11 experienced increased moisture compared to the Holocene in various global regions (Candy et al., 2014). Evidence of lake levels in Britain (Turner, 1970; Gibbard, 1977; Gibbard and Aalto, 1977; Gibbard et al., 1986; Boreham and Gibbard, 1995; Ashton et al., 2008) and geochemical data from tufa formations in France suggest regional shifts in rainfall patterns, possibly reflecting seasonality of rainfall, linked to the climatic peak of MIS 11c (Sherriff et al., 2021). During this particular substage, there was a significant increase in mixed oak forest and Mediterranean plant species. This expansion of forests, known as the 'Sines' forest phase in marine records along the Iberian margin (Oliveira et al., 2016; Hes et al., 2022), indicates the most pronounced warming and seasonal rainfall in the southwestern Mediterranean region. MIS 11 lacustrine deposits are consistently reported from the North Sahara (Geyh and Thiedig, 2008) and a contemporaneous humid phase is documented in the SW Libyan Sahara (Armitage et al., 2007).

In the Southwest Mediterranean, it has been observed that the typical Mediterranean vegetation gradually contracts during MIS 11, indicating the progressive influence of recurrent episodes of cooler and drier atmospheric conditions throughout MIS 11 (e.g., Oliveira et al., 2016). A number of events of abrupt forest decline indicate the gradual building up of colder and drier atmospheric conditions without concurrent variations in sea surface temperature (SST). All these events took place during transitions from periods of low ice volume, coinciding with the high sea levels of MIS 11c, to the transition from MIS 11c to MIS 11b, and ultimately to the end of MIS 11. The latter periods were marked by relatively weak ice sheet growth. During the MIS 11c/11b transition, an air-sea decoupling event occurred, highlighting the onset of the subsequent MIS 10 glacial phase, caused by increased moisture transport northward, thus accelerating the growth of the northern ice cap (e.g., Oliveira et al., 2016).

Particularly long, cold, dry, and windy events in Southwest Europe, along with a strong SST cooling, marked MIS 11b, an interval with higher ice volume conditions. These high-intensity events were contemporaneous with well-known and evident North Atlantic cooling events associated with iceberg discharges, likely originating from European ice caps. The dynamics of the northern ice caps were a key factor in amplifying the extent of precipitation and temperature reduction in SW Europe and prolonging the duration of these abrupt climatic changes.

The onset of climatic cooling subsequent to the peak of 400 ka during MIS 11 is sudden and very rapid, as highlighted by numerous MIS curves and associated sea level variation curves from marine (e.g., Lisiecki and Raymo, 2005; Grant et al., 2014) and terrestrial (Marra et al., 2021, 2022) records. This is followed by a progressive cooling, more gradual but constant and continuous, until the new cold peak of MIS 10.

Overall, the SU 7- SU 1 stratigraphic succession of Campo della Spina demonstrates a shift from relatively dry conditions at the base to progressively warmer and wetter conditions toward the top. A detailed analysis of this sequence reveals a progression: starting from arid (and possibly cooler) conditions, transitioning into an intermediate phase marked by periodic fluctuations between wet and dry cycles, and culminating in the establishment of more humid conditions, albeit with seasonal variations in water levels. These humid conditions facilitated the formation of a lake, where the elephant died either at its margins or within. The period of sustained warmth and increased precipitation during SU 3 gave way to a subsequent unstable phase characterized by alternating dry and moist conditions, favoring the development of a ferruginous duricrust. Subsequently, a renewed period of prolonged wet and warm conditions during SU 2 led to a resurgence in the water level in the basin.

The sequence at Campo della Spina tentatively suggests a succession of events that may correspond to the trends observed in high-resolution climatic reconstructions of the MIS 11c through MIS 11b transition. Evidence collected from the excavation at Campo della Spina indicates that the elephant died within or on the banks of a (ephemeral?) water basin. An initial lahar, probably triggered by intense and concentrated storms, possibly involving heavy downpours, engulfed the animal's already skeletonized carcass, under generally warm-moist tropical-like conditions. Several secondary volcanoclastic flow events followed the initial one, possibly indicating a series of violent and intense downpours, which may reflect an alternation of more rainy periods, interspersed with gradually drier episodes. A similar situation ultimately led to conditions favorable for the formation of the hard, iron-rich duricrust present at the site.

4.3. Biochronological considerations

The straight-tusked elephant *Palaeoloxodon antiquus* is recognized as a prominent species in extinct Italian large mammal assemblages, especially during the late Middle and early Late Pleistocene (Palombo and Ferretti, 2005). This taxon probably evolved from a *Palaeoloxodon recki*-type ancestor, which spread from Africa during the Early to Middle Pleistocene transition, as evidenced by the discovery of a partial skull at the Israeli site of Gesher Benot Ya'aqov (dated to 0.8 Ma, MIS 21) (cfr., Larramendi et al., 2020 and references therein).

During the period from 0.9 to 0.65 Ma, *Palaeoloxodon antiquus* was among the numerous herbivores that migrated into the Apennine Peninsula from the Asian steppe via Eastern Europe. This migration marked the species' integration into a diverse assemblage that replaced the declining Epivillafranchian fauna. Notable fossil sites such as Slivia, Monte Tenda, and Ponte Galeria 2 document the presence of *Palaeoloxodon antiquus* alongside other significant taxa (Kahlke et al., 2011). The first appearance of this species in Europe is recorded by an isolated but well-preserved molar discovered in the Slivia Italian local faunal assemblage (LFA), dated to shortly before the beginning of the Middle Pleistocene (ca. 0.8 Ma) (Palombo, 2014 and references therein).

In the Latium region, one of the earliest occurrences of *P. antiquus* is recorded in the Ponte Galeria area near Rome, particularly in the Cava Arnolfi and Muratella di Mezzo both dated to around 0.7 Ma (Marra et al., 2014 and references therein). At Ficoncella (Viterbo), dated to around 0.5 Ma, the oldest evidence of human-elephant interaction has been documented, including an elephant carcass associated with a small tools industry described by Aureli et al. (2015).

Contemporaneous sites with Campo della Spina, such as Castel di Guido, Malagrotta and Fontana Ranuccio, have yielded significant remains of *P. antiquus*, recently dated to around 0.4 Ma (Pereira et al., 2018; Villa et al., 2021). Here, elephant bones were used by Middle Pleistocene hominins to produce bone tools such as bifaces (Villa et al., 2021).

It is worth noting that nearly complete skeletons of *P. antiquus* were discovered in the 1940s and 1950s in diatomaceous layers near Grotte Santo Stefano (Viterbo) (Trevisan, 1948; Palombo and Villa, 2003) and Riano Flaminio (Maccagno, 1962; Palombo and Villa, 2003), although no lithic or bone artefacts were found at these sites. Evidence for *in situ* butchering of an elephant carcass by hominins has been reported from La Polledrara di Cecanibbio (Anzidei et al., 2012) and Castel di Guido (Boschian et al., 2019 and references within). As reported by Aureli et al. (2012), in the Latium area, the extent and condition of the findings associated with *P. antiquus* remains, along with Lower Paleolithic industries, are strongly influenced by depositional context and taphonomic factors.

Other sporadic remains of *P. antiquus* found in Latium are reported in Palombo and Ferretti (2005). The last confirmed occurrence of the straight-tusked elephant in the Italian Peninsula is from deposits dating to MIS 5, with *P. antiquus* remains reported in Balzi Rossi and Grimaldi cave deposits, which range from MIS 5 to MIS 3 (cf., Moussous et al., 2014). However, the stratigraphic position and age of the Grimaldi cave levels remain uncertain, and there is no compelling evidence of the species' presence in Italy beyond MIS 5a to MIS 4 (Braun and Palombo, 2012, and references therein).

During the MIS 11 interglacial, *Palaeoloxodon antiquus* emerged as a

key species in the "*antiquus*-gravels" of Steinheim and Heppenloch cave, both located in Baden-Württemberg. The Steinheim fauna, consisting largely of browsers and mixed feeders such as *Bos primigenius*, *Megaloceros giganteus antecedens*, *Cervus elaphus*, and *Stephanorhinus kirchbergensis*, indicates a predominantly forested environment (Adam et al., 1995). In contrast, the Heppenloch assemblage, which lacks species like the giant deer and forest rhino, suggests more open and less forested conditions (Adam, 1975). The presence of *Palaeoloxodon antiquus* in these fossil sites, alongside other species such as *Bubalus murrensis*, underscores the warm-humid climate of central Europe during this time (Berckhemer, 1927; Schertz, 1937; Schreiber and Munk, 2002).

5. Conclusions

The excavation at Campo della Spina has provided invaluable insights into the Middle Pleistocene geological and paleontological dynamics of central Italy. The fossiliferous sedimentary lens unearthed at the site, hosting well preserved skeletal remains of an adult *Palaeoloxodon antiquus*, offers a unique window into the interplay between climate dynamics, geological processes, paleoenvironments, and taphonomic factors.

The sedimentary succession at Campo della Spina represents a dynamic depositional environment influenced by fluctuating water levels, volcanic activity, and episodic sedimentary events. The coexistence of lacustrine features alongside debris flow attributes reflects a fluctuation from warmer, moister environments to drier conditions, and finally a return to warmer, wetter climates through the local stratigraphic sequence. Does this series of occurrences mirror the progression reported for the transition from MIS 11 to MIS 10 and the ensuing MIS 9 interglacial period?

The well-preserved remains of a *Palaeoloxodon antiquus* skeleton, along with the absence of weathering or carnivore activity on bone surfaces, suggests *in situ* death and subsequent burial in a protective environment. However, evidence of bone breakage and disarticulation indicates potential post-depositional disturbance, likely attributable to tractive water movements or debris flow events.

The preservation of the *Palaeoloxodon* remains also opens up possibilities for further investigation into the paleoecology of this species. Studies by Saarinen and Lister (2016) have demonstrated that mesowear analysis, which records the relief of worn molar surfaces, can serve as a dietary proxy, distinguishing between grazing and browsing diets in proboscideans. Applying such methods to the dental remains from Campo della Spina could provide valuable insight into the local vegetation and environmental conditions during the MIS 11 to MIS 9 interval. In particular, mesowear angles could reveal whether *Palaeoloxodon antiquus* at this site adapted to shifts in vegetation, such as periods of abundant grasses or a more mixed feeding strategy, as seen in other Pleistocene proboscideans.

Further, recent studies such as Foister et al. (2024) suggest that large herbivores, including proboscideans, played a significant role in shaping and responding to the ecosystems they inhabited. Their findings on Early Pleistocene mammalian communities indicate that proboscideans, through their flexible feeding strategies, could thrive in both grassy and wooded environments, adapting to diverse ecological contexts. Although the focus of Foister et al. (2024) is on earlier periods, their conclusions on ecological plasticity in large herbivores highlight the adaptability of species like *Palaeoloxodon*, which may have exhibited similar plasticity in the changing environments of the Middle Pleistocene.

Radiometric dating of volcanic deposits places the fossil-bearing succession within the MIS 11 – MIS 9 interval, particularly correlating with the substage MIS 11c. This interval, characterized by warm, humid conditions, holds relevance for understanding past climate dynamics and serves as a potential analog for future climate scenarios.

The similarities between MIS 11 and present climate trends raise intriguing questions regarding future climate trajectories. The potential for a rapid cooling event, analogous to transitions observed from MIS 11 to MIS 10, underscores the importance of understanding past climatic shifts for informing contemporary climate change mitigation strategies. Given the aforementioned similarities between MIS 11 and MIS 1, an intriguing question arises: does MIS 11 correspond to any ongoing phenomena in the current terrestrial climate? MIS 11 documents a contraction of typical Mediterranean vegetation and the occurrence of abrupt climatic changes, as discussed earlier in this study. Is this indicative of what awaits us in the near geological future?

A highly speculative and intriguing hypothesis suggests that in the course of MIS 1, the climate could transition to conditions similar to those observed during MIS 11, leading to a new cold peak. Indeed, respecting the dominant periodicity of the 100 ka glacial-interglacial oscillations, as recognized by Milanković, 1941 and characteristic since the Early to Middle Pleistocene transition (ca. 0.8–1.2 Ma), the warm peak of MIS 1 occurs approximately 100 ka after MIS 5e, which marks the beginning of the Late Pleistocene. Should the climate evolve as during MIS 11, an initially rapid cooling (on a geological timescale) can be anticipated, followed by a less rapid but steady progression. Based on the durations of the climatic plateaux of MIS 11 and MIS 9, which correspond to the documented high-stands in sequential stratigraphy, it can be speculated that the cooling following the peak of MIS 1 will occur in the near geological future. The climatic history of the past hints at the possibility that, akin to changes observed after the warm peak of the fossiliferous level of Campo della Spina, a sudden alteration potentially mitigating current global warming might occur in the (geologically) near future. Unfortunately, the timing of this event cannot be determined, and there is a great difference between a few years and a thousand years in terms of social and economic effects. However, the possibility of a short-term change exists, and perhaps there are ways to begin evaluating whether there are other indicators of proximity or otherwise. The occurrence of intense downpours and periods of severe drought, which we are experiencing during the current phase of global warming, may herald an increase in moisture transport towards higher latitudes and an acceleration of growth in the Arctic ice cap. This, of course, is contingent upon mitigating the interference of anthropogenic activities.

In summary, the findings from Campo della Spina contribute significantly to our understanding of Middle Pleistocene paleoenvironments, taphonomic processes, and climate dynamics. This research underscores the importance of interdisciplinary investigations in unraveling the complexities of Earth's past, while also highlighting the relevance of paleoclimate studies for addressing contemporary environmental challenges. Assembling small, irregularly shaped pieces like Campo della Spina into the vast jigsaw puzzle of the past helps to provide a clearer view of the climate's future.

CRediT authorship contribution statement

Paul P.A. Mazza: Writing – review & editing, Writing – original draft, Visualization, Validation, Supervision, Resources, Methodology, Investigation, Funding acquisition, Formal analysis, Data curation. **Fabrizio Marra:** Writing – review & editing, Writing – original draft, Supervision, Methodology, Investigation, Funding acquisition, Formal analysis, Data curation, Conceptualization. **Giovanni Maria Di Buduo:** Writing – review & editing, Investigation, Data curation, Conceptualization. **Luca Bellucci:** Writing – review & editing, Writing – original draft. **Mirko Bonechi:** Writing – original draft, Methodology, Formal analysis, Data curation. **Ezra Goemans:** Writing – original draft, Methodology, Formal analysis, Data curation. **Cosimo Bonechi:** Writing – original draft, Methodology, Formal analysis, Data curation. **Luca Costantini:** Writing – review & editing, Investigation. **Sebastien Nomade:** Writing – review & editing, Methodology, Investigation, Data curation. **Danilo M. Palladino:** Writing – review & editing, Methodology, Investigation, Data curation. **Alison Pereira:** Writing – review & editing, Methodology, Investigation, Data curation. **Andrea Savorelli:**

Writing – review & editing, Investigation, Data curation.

Data availability

The full analytical data for the 40Ar/39Ar dating of single grains is available in Supplementary Dataset 1 (SD-1).

Funding

P.P.A.M. was supported in the present study by PAULMAZZARICATEN24– Mazza P. Fondo Ateneo 2024 MIUR (the Italian Ministry of Education, Universities and Research) grant.

Declaration of competing interest

The authors declare that they have no known competing financial interests or personal relationships that could have appeared to influence the work reported in this paper.

Acknowledgments

The authors gratefully acknowledge the generous support of Archeologica Castel Cellesi, alongside Antonio and Giorgio Melani, for their contributions to the funding of the Campo della Spina excavation. Their invaluable assistance and unwavering support were instrumental in the success of the 2014 excavation as well as to the present research endeavor. Special thanks are extended to Carla Porchiella, Brunella Ceccantoni, and Valerio Pecci for their outstanding assistance and warm hospitality during the course of the excavation. Their dedication and professionalism greatly facilitated the progress of the project.

The writers extend their sincere gratitude to Maria Letizia Arancio of the Superintendence for Southern Etruria the metropolitan area of Rome for her invaluable support and assistance throughout the course of the excavation. More generally, the authors express their gratitude to the Italian Ministry of Culture (MiC) – Superintendence for Archaeology, Fine Arts, and Landscape for the Province of Viterbo and Southern Etruria for its kind collaboration and assistance.

The authors also wish to express their gratitude to all the students who participated in the summer school associated with the excavation. Their enthusiasm and hard work not only enriched the research experience but also contributed to the funding of the summer school.

The authors extend their sincere appreciation to the Mayor and Municipality of Bagnoregio for their valuable interest and support.

Furthermore, the authors would like to thank the university researchers Mauro Coltorti, Giorgio Manzi, Jacopo Cecchi Moggi, Maria Rita Palombo, and Pierluigi Pieruccini for their invaluable contributions to the summer school. Their insightful lessons and guidance greatly enhanced the educational aspect of the program.

Lastly, sincere appreciation is extended to the retired Museum technician Vittorio Borselli as well as to the Department of Earth Sciences' retired technician Francesco Landucci for their contributions to the summer school. Their expertise and mentorship played a significant role in ensuring the success of the program.

Appendix A. Supplementary data

Supplementary data to this article can be found online at https://doi.org/10.1016/j.quaint.2024.10.014.

References

Acocella, V., Palladino, D.M., Cioni, R., Russo, P., Simei, S., 2012. Caldera structure, amount of collapse and erupted volumes: the case of Bolsena Caldera, Italy. Geol. Soc. Am. Bull. 124 (1), 1562–1576. https://doi.org/10.1130/B30662, 9-10.

Adam, K.D., 1975. Die mittelpleistozäne Säugetier-Fauna aus dem Heppenloch bei Gutenberg (Württemberg) Stuttgarter Beiträge zur Naturkunde B, vol. 3, pp. 1–247.

Adam, K.D., Bloos, G., Ziegler, R., 1995. In: Schirmer, W. (Ed.), Quaternary Field Trips in Central Europe, Vol. 2, Field Trips on Special Topics. Verlag Dr. Friedrich Pfeil, München, pp. 726–728. Steinheim/Murr, N of Stuttgart – Locality of *Homo steinheimensis*.

Anemone, R.L., Conroy, G.C., Emerson, C.W., 2011. GIS and paleoanthropology: incorporating new approaches from the geospatial sciences in the analysis of primate and human evolution. Am. J. Phys. Anthropol. 146 (S53), 19–46. https://doi.org/10.1002/ajpa.21609.

AnzideI, A.P., Bulgarelli, G.M., Catalano, P., Cerilli, E., Gallotti, R., Lemorini, C., Milli, S., Palombo, M.R., Pantano, W., Santucci, E., 2012. Ongoing research at the late Middle Pleistocene site of La Polledrara di Cecanibbio (central Italy), with emphasis on human–elephant relationships. Quat. Int. 255, 171–187. https://doi.org/10.1016/j.quaint.2011.06.005.

Armitage, S.J., Drake, N.A., Stokes, S., El-Hawat, A., Salem, M.J., White, K., Turner, P., McLaren, S.J., 2007. Multiple phases of north african humidity recorded in lacustrine sediments from the fazzan basin, Libyan Sahara. Quat. Geochronol. 2 (1–4), 181–186. https://doi.org/10.1016/j.quageo.2006.05.019.

Ashton, N.M., 2010. Challenges to the Occupation of North-West Europe during the Late Middle Pleistocene. Dissertation Leiden University.

Ashton, N., Lewis, S.G., Parfitt, S.A., Penkman, K.E.H., Coope, G.R., 2008. New evidence for complex climate change in MIS 11 from Hoxne, Suffolk, UK. Quat. Sci. Rev. 27, 652–668. https://doi.org/10.1016/j.quascirev.2008.01.003.

Aureli, D., Contardi, A., Giaccio, B., Modesti, V., Palombo, M.R., Rozzi, R., Sposato, A., Trucco, F., 2012. Straight-tusked elephants in the Middle Pleistocene of northern Latium: preliminary report on the ficoncella site (tarquinia, central Italy). Quat. Int. 255, 29–35. https://doi.org/10.1016/j.quaint.2011.06.052.

Aureli, D., Contardi, A., Giaccio, B., Jicha, B., Lemorini, C., Madonna, S., Magri, D., Marano, F., Milli, S., Modesti, V., Palombo, M.R., Rocca, R., 2015. *Palaeoloxodon* and human interaction: depositional setting, chronology and archaeology at the Middle Pleistocene Ficoncella site (Tarquinia, Italy). PLoS One 10 (4), e0124498. https://doi.org/10.1371/journal.pone.0124498.

Balbas, A., Koppers, A.A.P., Kent, D.V., Konrad, K., Clark, P.U., 2016. Identification of the short-lived santa rosa geomagnetic excursion in lavas on floreana island (galapagos) by 40Ar/39Ar geochronology. Geology 44 (5), 359–362. https://doi.org/10.1130/G37569.1.

Behrensmeyer, A.K., 1978. Taphonomic and ecologic information from bone weathering. Paleobiology 4 (2), 150–162. https://doi.org/10.1017/S0094837300005820.

Berger, A., Loutre, M.F., 2002. An exceptionally long interglacial ahead? Science 297, 1287–1288. https://doi.org/10.1126/science.1076120.

Berckhemer, F., 1927. *Buffelus murrensis* n. sp. Ein diluvialer Büffelschädel von Steinheim ad Murr. Jahreshefte des Vereins für vaterländische Naturkunde in Württemberg 83, 146–158.

Blain, H.A., Fagoaga, A., Ruiz-Sánchez, F.J., Garcia-Medrano, P., Olle, A., Jiménez-Arenas, J.M., 2021. Coping with arid environments: a critical threshold for human expansion in Europe at the Marine Isotope Stage 12/11 transition? The case of the Iberian Peninsula. J. Hum. Evol. 153, 102950. https://doi.org/10.1016/j.jhevol.2021.102950.

Blueweiss, L., Fox, H., Kudzma, V., Nakashima, D., Peters, R., Sams, S., 1978. Relationships between body size and some life history parameters. Oecologia 37, 257–272. https://doi.org/10.1007/BF00344996.

Boreham, S., Gibbard, P.L., 1995. Middle Pleistocene hoxnian stage interglacial deposits at hitchin, hertfordshire, england. Proc. Geol. Assoc. 106 (4), 259–270. https://doi.org/10.1016/S0016-7878(08)80237-4.

Boschian, G., Caramella, D., Saccà, D., Barkai, R., 2019. Are there marrow cavities in Pleistocene elephant limb bones, and was marrow available to early humans? New CT scan results from the site of Castel di Guido (Italy). Quat. Sci. Rev. 215, 86–97. https://doi.org/10.1016/j.quascirev.2019.05.010.

Boschin, F., Rocca, R., Aureli, D., 2018. New archaeozoological and taphonomic analysis on macro-and megafauna remains from the Lower Palaeolithic site of Ficoncella (Tarquinia, Central Italy). Quaternaire. Revue de l'Association française pour l'étude du Quaternaire 29 (1), 13–20.

Braun, I.M., Palombo, M.R., 2012. *Mammuthus primigenius* in the cave and portable art: an overview with a short account on the elephant fossil record in Southern Europe during the last glacial. Quat. Int. 276, 61–76. https://doi.org/10.1016/j.quaint.2012.07.010.

Brocchi, G.B., 1816. Lettera sopra alcuni ammassi colonnari basaltini del territorio di Viterbo. Biblioteca Italia. III, 495–507.

Campana, S., Sordini, M., Bianchi, G., Fichera, G.A., Lai, L., 2012. 3D recording and total archaeology: from landscapes to historical buildings. IJHDE 1 (3), 443–460.

Candy, I., Schreve, D.C., Sherriff, J., Tye, G.J., 2014. Marine Isotope Stage 11: palaeoclimates, palaeoenvironments and its role as an analogue for the current interglacial. Earth Sci. Rev. 128, 18–51. https://doi.org/10.1016/j.earscirev.2013.09.006.

Ciampini, G.C., 1688. Ossa fossili di Vitorchiano nel Viterbese. Roma.

Clerici, E., 1895. Per la storia del sistema vulcanico vulsinio. Rend. Reg. Acc. Lincei 4, 219–226.

Clerici, E., 1908. Appunti per una escursione geologica a Viterbo. Boll. Soc. Geol. It. XXVII, 311–336.

Cox, S.E., Hemming, S.R., Tootell, D., 2020. The isotopx NGX and ATONA faraday amplifiers. Geochronology 2, 231–243. https://doi.org/10.5194/gchron-2-231-2020.

Davies, P., 2002. *The Straight-Tusked Elephant (*Palaeoloxodon Antiquus*) in Pleistocene Europe*. Master Thesis. University College London.

de Abreu, L., Abrantes, F.F., Shackleton, N.J., Tzedakis, P.C., McManus, J.F., Oppo, D.W., Hall, M.A., 2005. Ocean climate variability in the eastern North Atlantic during

interglacial marine isotope stage 11: a partial analogue for the Holocene? Paleoceaongraphy 20, PA3009, 101292004PA001091.

Di Buduo, G.M., Costantini, L., Fiore, I., Marra, F., Palladino, D.M., Petronio, C., Rolfo, M. F., Salari, L., Ceruleo, P., Gaeta, M., Gatta, M., Florindo, F., Modesti, V., Pandolfi, L., Sottili, G., 2020. The Bucobello 322 ka-fossil-bearing volcanoclastic-flow deposit in the eastern Vulsini volcanic district (central Italy): mechanism of emplacement and insights on human activity during MIS 9. Quat. Int. 554, 75–89. https://doi.org/10.1016/j.quaint.2020.04.046.

Dickson, A.J., Beer, C.J., Dempsey, C., Maslin, M.A., Bendle, J.A., McClymont, E.L., Pancost, R.D., 2009. Oceanic forcing of the marine isotope stage 11 interglacial. Nat. Geosci. 2 (6), 428–433.

Droxler, A.W., Alley, R.B., Howard, W.R., Poore, R.Z., Burckle, L.H., 2003. Unique and exceptionally long interglacial Marine Isotope Stage 11: window into Earth warm future climate. In: Droxler, A.W., Poore, R.Z., Burckle, L.H. (Eds.), Earth's Climate and Orbital Eccentricity: the Marine Isotope Stage 11 Question, vol. 137. Geophysical Monograph Series, pp. 1–14.

EPICA community members, 2004. Eight glacial cycles from an Antarctic ice core. Nature 429, 623–628.

Fawcett, P.J., Werne, J.P., Anderson, R.S., Heikoop, J.M., Brown, E.T., Berke, M.A., Smith, S.J., Goff, F., Donohoo-Hurley, L., Cisneros-Dozal, L.M., Schouten, S., Sinninghe Damsté, J.S., Huang, Y., Toney, J., Fessenden, J., WoldeGabriel, G., Atudorei, V., Geissman, J.W., Allen, C.D., 2011. Extended megadroughts in the southwestern United States during Pleistocene interglacials. Nature 470 (7335), 518–521.

Foister, T.I., Liu, L., Saarinen, J., Tallavaara, M., Zhang, H., Žliobaitė, I., 2024. Quantifying heterogeneity of hominin environments in and out of Africa using herbivore dental traits. Quat. Sci. Rev. 337, 108791. https://doi.org/10.1016/j.quascirev.2024.108791.

Geyh, M.A., Thiedig, F., 2008. The Middle Pleistocene Al Mahruqah Formation in the Murzuq Basin, northern Sahara, Libya evidence for orbitally-forced humid episodes during the last 500,000 years. Palaeogeogr. Palaeoclimatol. Palaeoecol. 257, 1–21.

Ghilani, C.D., 2010. Adjustment Computations: Spatial Data Analysis. John Wiley & Sons.

Gibbard, P.L., 1977. Pleistocene history of the vale of St.Albans. Philos. Trans. R. Soc. B 280, 445–483.

Gibbard, P.L., Aalto, M.M., 1977. A hoxnian interglacial site at Fishers green, stevenage, hertfordshire. New Phytol. 72, 505–523.

Gibbard, P.L., Bryant, I.D., Hall, A.R., 1986. A hoxnian interglacial doline infilling at slade oak lane, denham, buckinghamshire, england. Geol. Mag. 123 (1), 27–43.

Göhlich, U.B., 1998. Elephantoidea (Proboscidea, Mammalia) aus dem Mittel- und Obermiozän der Oberen Süßwassermolasse Süddeutschlands: Odontologie und Osteologie. Münchn. Geowiss. Abh. 36, 1–245.

Grant, K., Rohling, E., Ramsey, C.B., Cheng, H., Edwards, R., Florindo, F., Heslop, D., Marra, F., Roberts, A., Tamisiea, M.E., 2014. Sea-level variability over five glacial cycles. Nat. Commun. 5, 5076.

Harris, E.C., 2014. Principles of Archaeological Stratigraphy. Elsevier.

Haynes, G., 1983. Frequencies of spiral and green-bone fractures on ungulate limb bones in modern surface assemblages. Am. Antiq. 48 (1), 102–114.

Haynes, G., 2017. Taphonomy of the Inglewood mammoth (*Mammuthus columbi*) (Maryland, USA): green-bone fracturing of fossil bones. Quat. Int. 445, 171–183.

Held, C., 2012. Creating 3D Models of Cultural Heritage Sites with Terrestrial Laser Scanning and 3D Imaging. Master's Thesis, University of Cape Town, South Africa.

Hes, G., Sánchez Goñi, M.F., Bouttes, N., 2022. Impact of terrestrial biosphere on the atmospheric CO_2 concentration across Termination V. Clim. Past 18 (6), 1429–1451.

Kandiano, E.S., Bauch, H.A., Fahl, K., Helmke, J.P., Röhl, U., Pérez-Folgado, M., Cacho, I., 2012. The meridional temperature gradient in the eastern North Atlantic during MIS 11 and its link to the ocean–atmosphere system. Palaeogeogr. Palaeoclimatol. Palaeoecol. 333, 24–39.

Kahlke, R.D., García, N., Kostopoulos, D.S., Lacombat, F., Lister, A.M., Mazza, P.P., et al., 2011. Western Palaearctic palaeoenvironmental conditions during the Early and early Middle Pleistocene inferred from large mammal communities, and implications for hominin dispersal in Europe. Quat. Sci. Rev. 30 (11–12), 1368–1395.

Kleinen, T., Hildebrandt, S., Prange, M., Rachmayani, R., Muller, S., Bezrukova, E., Brovkin, V., Tarasov, P.E., 2014. The climate and vegetation of Marine Isotope Stage 11 – model results and proxybased reconstructions at global and regional scale. Quat. Int. 348, 247–265.

Koppers, A.A.P., 2002. ArArCALC—software for $^{40}Ar/^{39}Ar$ age calculations. Comput. Geosci. 28, 605–619.

Larramendi, A., 2016. Shoulder height, body mass, and shape of proboscideans. Acta Palaeontol. Pol. 61, 537–574.

Larramendi, A., Zhang, H., Palombo, M.R., Ferretti, M.P., 2020. The evolution of *Palaeoloxodon* skull structure: disentangling phylogenetic, sexually dimorphic, ontogenetic, and allometric morphological signals. Quat. Sci. Rev. 229, 106090.

Laws, R.M., 1966. Age criteria for the african elephant. Afr. J. Ecol. 4, 1–37.

Lee, J.Y., Marti, K., Severinghaus, J.P., Kawamura, K., Yoo, H.S., Lee, J.B., Kim, J.S., 2006. A redetermination of the isotopic abundances of atmospheric Ar. Geochem. Cosmochim. Acta 70 (17), 4507–4512.

Lisiecki, L.E., Raymo, M.E., 2005. A Pliocene-Pleistocene stack of 57 globally distributed benthic $\delta^{18}O$ records. Paleoceanography 20, PA1003. https://doi.org/10.1029/2004PA001071.

Lister, A.M., 1994. Skeletal associations and bone maturation in the Hot Springs mammoths. In: Agenbroad, L.D., Mead, J.I. (Eds.), The Hot Springs Mammoth Site: a Decade of Field and Laboratory Research in Paleontology, Geology and Paleoecology. Mammoth Site Inc., pp. 253–268

Lister, A.M., 1999. Epiphyseal fusion and postcranial age determination in the woolly mammoth, *Mammuthus primigenius*. Deinsea 6, 79–88.

Lister, A.M., 2021. Quantitative analysis of mammoth remains from lynford, norfolk, england. In: Neanderthals among Mammoths: Excavations at Lynford Quarry, Norfolk, Boismier, W. A., Gamble, C., Coward, F. Eds. English Heritage Archaeological Reports, pp. 205–214.

Lister, A.M., Dimitrijević, V., Marković, Z., Knežević, S., Mol, D., 2012. A skeleton of 'steppe' mammoth (*Mammuthus trogontherii* Pohlig) from Drmno, near Kostolac, Serbia. Quat. Int. 276–277, 129–144. https://doi.org/10.1016/j.quaint.2012.03.021.

Lister, A.M., Stuart, A.J., 2010. The West Runton mammoth (*Mammuthus trogontherii*) and its evolutionary significance. Quat. Int. 228, 180–209.

Loutre, M.F., Berger, A., 2003. Marine Isotope Stage 11 as an analogue for the present interglacial. Global Planet. Change 36, 209–217.

Ludwig, K.R., 2003. Mathematical–statistical treatment of data and errors for 230Th/U geochronology. Rev. Mineral. Geochem. 52 (1), 631–656.

Maccagno, A.M., 1962. L' *Elephas antiquus* di Riano, Roma. Geol. Rom. I, 77–131.

Mancini, M., Girotti, O., Cavinato, G.P., 2004. Il Pliocene e il Quaternario della Media Valle del Tevere (Appennino Centrale). Geol. Rom. 37, 175–236.

Marano, F., Palombo, M.R., 2014. A reappraisal of the straight-tusked elephant from Grotte Santo Stefano (Viterbo, central Italy) kept in the Museum of palaeontology of sapienza university of Rome (Italy). Sci. Anna. School Geol. Speci. 102, 114.

Marra, F., Nomade, S., Pereira, A., Petronio, C., Salari, L., Sottili, G., Bahain, J.-J., Boschian, G., Di Stefano, G., Falguères, C., Florindo, F., Gaeta, M., Giaccio, B., Masotta, M., 2018. A review of the geologic sections and the faunal assemblages of Aurelian Mammal Age of Latium (Italy) in the light of a new chronostratigraphic framework. Quat. Sci. Rev. 181, 173–199.

Marra, F., Pandolfi, L., Petronio, C., Di Stefano, G., Gaeta, M., Salari, L., 2014. Reassessing the sedimentary deposits and vertebrate assemblages from Ponte Galeria area (Rome, central Italy): an archive for the Middle Pleistocene faunas of Europe. Earth Sci. Rev. 139, 104–122. https://doi.org/10.1016/j.earscirev.2014.08.014.

Marra, F., Costantini, L., Di Buduo, G.M., Florindo, F., Jicha, B.R., Monaco, L., Palladino, D.M., Sottili, G., 2019. Combined glacio-eustatic forcing and volcano-tectonic uplift: geomorphological and geochronological constraints on the Tiber River terraces in the eastern Vulsini Volcanic District (central Italy). Global Planet. Change 182, 103009. https://doi.org/10.1016/j.gloplacha.2019.103009, 2019.

Marra, F., Jicha, B.R., Palladino, D.M., Gaeta, M., Costantini, L., Di Buduo, G.M., 2020a. $^{40}Ar/^{39}Ar$ single crystal dates from pyroclastic deposits provide a detailed record of the 590-240 ka eruptive period at the Vulsini Volcanic District (central Italy). J. Volcanol. Geoth. Res. 398, 106904. https://doi.org/10.1016/j.jvolgeores.2020.106904.

Marra, F., Castellano, C., Cucci, L., Florindo, F., Gaeta, M., Jicha, B., Palladino, D.M., Sottili, G., Tertulliani, A., Tolomei, C., 2020b. Monti sabatini and colli albani: the dormant twin volcanoes at the gates of Rome. Sci. Rep. 10, 8666. https://doi.org/10.1038/s41598-020-65394-2.

Marra, F., Pereira, A., Boschian, G., Nomade, S., 2021. MIS 13 and MIS 11 aggradational successions of the Paleo-Tiber delta: geochronological constraints to sea-level fluctuations and to the Acheulean sites of Castel di Guido and Malagrotta (Rome, Italy). Quat. Int. 616, 1–11. https://doi.org/10.1016/j.quaint.2021.12.016.

Marra, F., Pereira, A., Jicha, B., Nomade, S., Bidditu, I., Florindo, F., Muttoni, G., Niespolo, E.M., Renne, P.R., Scao, V., 2022. Terrestrial records of glacial termination V and IV and insights on deglacial mechanisms. Sci. Rep. 12, 18770. https://doi.org/10.1038/s41598-022-23391-7.

Mazza, P., 2014. Paleontology spring field school report on the excavation of Castel Cellesi (Bagnoregio, Viterbo, Central Italy). Alp. Mediterr. Quat. 27 (1), xi–xvii.

Melles, M., Brigham-Grette, J., Minyuk, P.S., Nowaczyk, N.R., Wennrich, V., DeConto, R. M., Anderson, P.M., Andreev, A.A., Coletti, A., Cook, T.L., Haltia-Hovi, E., Kukkonen, M., Lozhkin, A.V., Rosen, P., Tarasov, P., Vogel, H., Wagner, B., 2012. 2.8 million years of Arctic climate change from Lake El'gygytgyn, NE Russia. Science 337, 315–320.

Milanković, M., 1941. Kanon der Erdbestrahlung und seine Anwendung auf des Eiszeitenproblem. In: Special Publication 132, Section of Mathematical and Natural Sciences Royal Serbian Academy of Sciences, Belgrade, Serbia, 33, pp. 1–633.

Monaco, L., Palladino, D.M., Gaeta, M., Marra, F., Sottili, G., Leicher, N., Mannella, G., Nomade, S., Pereira, A., Regattieri, E., Wagner, B., Zanchetta, G., Albert, P.G., Arienzo, I., D'Antonio, M., Petrosino, P., Giaccio, B., 2021. Mediterranean tephrostratigraphy and peri-Tyrrhenian explosive activity over the 430-365 ka interval: a new benchmark data from Fucino basin. Earth Sci. Rev. 220, 103706. https://doi.org/10.1016/j.earscirev.2021.103706.

Moussous, A., Valensi, P., Simon, P., 2014. Identification de l'ivoire de Proboscidiens des grottes des Balzi Rossi (Ligurie, Italie) à partir de la méthode des lignes de Schreger. Bulletin Mus. Anthropol. préhist. Monaco 54, 83–90.

Mumtaz, S.A., 2008. Integrating terrestrial laser scanning models into 3d Geodatabase. In: 2008 2nd International Conference on Advances in Space Technologies. IEEE, pp. 124–130.

Niespolo, E.M., Rutte, D., Deino, A.L., Renne, P.R., 2017. Intercalibration and age of the Alder Creek sanidine 40Ar/39Ar standard. Quat. Geochronol. 39, 205–213.

Oliveira, D., Desprat, S., Rodrigues, T., Naughton, F., Hodell, D., Trigo, R., Rufino, M., Lopes, C., Abrantes, F., Goni, M.F.S., 2016. The complexity of millennial-scale variability in southwestern Europe during MIS 11. Quat. Res. 86 (3), 373–387.

Palladino, D.M., Simei, S., Sottili, G., Trigila, R., 2010. Integrated approach for the reconstruction of stratigraphy and geology of Quaternary volcanic terrains: an application to the Vulsini Volcanoes (central Italy). In: Groppelli, G., Viereck-Goette, L. (Eds.), Stratigraphy and Geology of Volcanic Areas, vol. 464. The Geological Society of America Special Paper, pp. 63–84.

Palombo, M.R., 2014. Deconstructing mammal dispersals and faunal dynamics in SW Europe during the Quaternary. Quat. Sci. Rev. 96, 50–71.

Palombo, M.R., Ferretti, M.P., 2005. Elephant fossil record from Italy: knowledge, problems, and perspectives. Quat. Int. 126, 107–136.

Palombo, M.R., Villa, P., 2003. Sexually dimorphic characters of Elephas (*Palaeoloxodon) antiquus* from Grotte Santo Stefano (Viterbo, Central Italy). Deinsea 9 (1), 293–316.

Pianciani, G.B., 1817. Delle ossa fossili di Magognano nel territorio di Viterbo. Opuscoli scientifici di Bologna. Annesio Nobili Ed, pp. 345–356.

Pereira, A., Nomade, S., Moncel, M.H., Voinchet, P., Bahain, J.J., Biddittu, I., Falguères, C., Giaccio, B., Manzi, G., Parenti, F., Scardia, G., Scao, V., Sottili, G., Vietti, A., 2018. Integrated geochronology of Acheulian sites from the southern Latium (central Italy): insights on human-environment interaction and the technological innovations during the MIS 11-MIS 10 period. Quat. Sci. Rev. 187, 112–129.

Prokopenko, A.A., Karabanov, E.B., Williams, D.F., Kuzmin, M.I., Shackleton, N.J., Crowhurst, S.J., Peck, J.A., Gvozdkov, A.N., King, J.W., 2001. Biogenic silica record of the Lake Baikal response to climatic forcing during the Brunhes. Quat. Res. 55 (2), 123–132.

Railsback, L.B., Gibbard, P.L., Head, M.J., Voarintsoa, N.R.G., Toucanne, S., 2015. An optimized scheme of lettered marine isotope substages for the last 1.0 million years, and the climatostratigraphic nature of isotope stages and substages. Quat. Sci. Rev. 111, 94–106.

Rensch, B., 1959. Evolution above the Species Level. Columbia University Press.

Roth, V.L., 1984. How elephants grow: heterochrony and the calibration of developmental stages in some living and fossil species. J. Vertebr. Paleontol. 4, 126–145.

Saarinen, J., Lister, A.M., 2016. Dental mesowear reflects local vegetation and niche separation in Pleistocene proboscideans from Britain. J. Quat. Sci. 31 (7), 799–808. https://doi.org/10.1002/jqs.2906.

Sassoon, D., Lebreton, V., Combourieu-Nebout, N., Peyron, O., Moncel, M.H., 2023. Palaeoenvironmental changes in the southwestern Mediterranean (ODP site 976, Alboran sea) during the MIS 12/11 transition and the MIS 11 interglacial and implications for hominin populations. Quat. Sci. Rev. 304, 108010.

Schertz, E., 1937. Ein neuer Wasserbüffel aus dem Diluvium Mitteldeutschlands (Buffelus wanckeli nov. spec.). Paläont. Z. 19, 57–72.

Sherriff, J.E., Schreve, D.C., Candy, I., Palmer, A.P., White, T.S., 2021. Environments of the climatic optimum of MIS 11 in Britain: evidence from the tufa sequence at Hitchin, southeast England. J. Quat. Sci. 36 (4), 508–525.

Schreiber, H.D., Munk, W., 2002. A skull fragment of *Bubalus murrensis* (berckhemer, 1927) (mammalia, bovinae) from the Pleistocene of bruchsal-buchenau (NE-Karlsruhe, SW-Germany). Neues Jahrbuch Geol. Palaontol. Monatsh. 2002, 737–748.

Trevisan, L., 1948. Lo scheletro di *Elephas antiquus italiquus* di Fonte Campanile (Viterbo). Palaeontogr. Ital. 44, 2–78, 1949.

Turner, C., 1970. The Middle Pleistocene deposits at marks tey, essex. Philos. Trans. R. Soc. B, Biol. Sci. 257 (817), 373–437.

Tzedakis, P.C., 2010. The MIS 11–MIS 1 analogy, southern European vegetation, atmospheric methane and the "early anthropogenic hypothesis". Clim. Past 6 (2), 131–144.

Tzedakis, P.C., Andrieu, V., De Beaulieu, J.L., Birks, H.J.B., Crowhurst, S., Follieri, M., Hooghiemstra, H., Magri, D., Reille, M., Sadori, L., Shackleton, N.J., Wijmstra, T.A., 2001. Establishing a terrestrial chronological framework as a basis for biostratigraphical comparisons. Quat. Sci. Rev. 20 (16–17), 1583–1592.

Tzedakis, P.C., Channell, J.E.T., Hodell, D.A., Kleiven, H.F., Skinner, L.C., 2012. Determining the natural length of the current interglacial. Nat. Geosci. 5 (2), 138–141.

Tzedakis, P.C., Hodell, D.A., Nehrbass-Ahles, C., Mitsui, T., Wolff, E.W., 2022. Marine isotope stage 11c: an unusual interglacial. Quat. Sci. Rev. 284, 107493.

Vallance, J.W., 2005. Volcanic debris flows. In: Debris Flow Hazards and Related Phenomena, Jakob, Matthias, and Hungr, Oldrich. Springer-Praxis, Heidelberg, pp. 247–274.

Villa, P., Mahieu, E., 1991. Breakage patterns of human long bones. J. Hum. Evol. 21 (1), 27–48.

Villa, P., Boschian, G., Pollarolo, L., Saccà, D., Marra, F., Nomade, S., Pereira, A., 2021. Elephant bones for the Middle Pleistocene toolmaker. PLoS One 16 (8), e0256090.

Westaway, R., 2010. Improved age constraint for pre-and post-Anglian temperate-stage deposits in north Norfolk, UK, from analysis of serine decomposition in *Bithynia* opercula. J. Quat. Sci. 25 (5), 715–723.

Williams, M., 2019. The Nile Basin: Quaternary Geology, Geomorphology and Prehistoric Environments. Cambridge University Press.

Zhao, X., Cheng, H., Sinha, A., Zhang, H., Baker, J.L., Chen, S., Kong, X., Wang, Y., Edwards, R.L., Ning, Y., Zhao, J., 2019. A high-resolution speleothem record of Marine Isotope Stage 11 as a natural analog to Holocene Asian summer monsoon variations. Geophys. Res. Lett. 46 (16), 9949–9957.